

Experimental observation of charge ordering in nanocrystalline $\text{Pr}_{0.65}\text{Ca}_{0.35}\text{MnO}_3$

Anis Biswas and I. Das

Saha Institute of Nuclear Physics, 1/AF, Bidhannagar, Kolkata 7000 064, India

(Received 15 May 2006; revised manuscript received 7 September 2006; published 9 November 2006)

Observation of charge ordering in single crystalline and bulk polycrystalline systems of various rare-earth based manganites is well documented. However, there is hardly any manifestation of the same when the grain size is reduced to nanoscale. We have observed charge ordering in the case of nanocrystalline $\text{Pr}_{0.65}\text{Ca}_{0.35}\text{MnO}_3$ of average particle size 40 nm. This phenomenon is attributed to the primary role played by the martensitic character of the charge order transition in the material.

DOI: [10.1103/PhysRevB.74.172405](https://doi.org/10.1103/PhysRevB.74.172405)

PACS number(s): 75.47.Lx, 73.63.Bd

I. INTRODUCTION

The phenomenon charge ordering (CO) in perovskite manganites with the general formula $R_{1-x}B_x\text{MnO}_3$ (where R is rare-earth and B is bivalent ion) has become a subject of intense research.^{1,2} This intriguing phenomenon is associated with strong interplay between charge, lattice, and orbital degrees of freedom and mainly observed for some commensurate fraction of carrier concentration, such as $x = 1/2, 2/3, 4/5$, etc. However, the formation of CO state is also possible for other incommensurate values of carrier concentration. CO state can be destabilized by magnetic field and gives rise to a large negative magnetoresistance (MR). In literature, there are many studies regarding CO in polycrystalline and single crystalline bulk form of the sample.^{1,2} The primary ingredients behind the formation of CO state are emphasized as the competition between double exchange (DE) and super exchange (SE) among the core spins of manganese and the Coulomb interaction between electrons of different orbitals of the same manganese site.^{3,4} The charge order transition is accompanied by structural transition. This structural effect has been considered as the secondary effect of CO. More recently, the polarized optical studies have revealed that CO is a martensitic-like transformation.⁵ The martensitic strain is another important factor in the case of CO.⁵⁻⁷ The phenomenon CO is not explored much in case of a nanocrystalline form of the samples. The issue is still not clear of which factor plays the dominant role in CO, especially when the particle size of the system is reduced. In this Brief Report, our primary objective is to address this issue by studying the phenomenon in nanocrystalline material.

The Ca-doped Pr manganites ($\text{Pr}_{1-x}\text{Ca}_x\text{MnO}_3$) with the doping concentration $0.3 \leq x \leq 0.5$ in bulk form show the same generic behavior in their phase diagram.⁸ They remain at insulating state in all temperatures in absence of any external perturbation. Charge order transition occurs below a certain temperature (T_{CO}).⁸ The antiferromagnetic transition does not coincide with CO. The antiferromagnetic transition temperature, T_N , is always less than T_{CO} .⁸ For the samples having Ca concentration away from commensurate value “0.5,” the antiferromagnetic state is transformed to a canted antiferromagnetic state at low temperature well below T_N .⁸

We have performed a detailed experimental study on the nanocrystalline $\text{Pr}_{0.65}\text{Ca}_{0.35}\text{MnO}_3$ of average particle size ~ 40 nm and CO state has been observed. In case of the bulk

$\text{Pr}_{0.65}\text{Ca}_{0.35}\text{MnO}_3$, T_{CO} and T_N are 225 K and 175 K, respectively.⁹ The canted antiferromagnetic structure has been stabilized below ~ 100 K.⁹

II. SAMPLE PREPARATION AND CHARACTERIZATION

The nanoparticles of $\text{Pr}_{0.65}\text{Ca}_{0.35}\text{MnO}_3$ have been prepared by a sol-gel technique. At the end of the process, the gel is decomposed at about 100°C and a porous black powder has been obtained. The powder is given heat treatment at 1000°C for 6 h to get a nanocrystalline sample. The x-ray diffraction study has confirmed the single phase nature of the sample with orthorhombic crystal structure ($pbnm$ symmetry) similar to the bulk sample.¹⁰ The values of the lattice constants ($a=5.420$ Å, $b=5.449$ Å, and $c=7.660$ Å) of the sample agree quite well with literature values for the bulk sample.¹⁰ Transmission electron microscopy (TEM) study has revealed that the average particle size is ~ 40 nm. One typical electron micrograph of the sample has been shown in Fig. 1. The histogram showing particle size distribution as well as the high-resolution transmission electron microscopy (HRTEM) image of the inside portion of a particle has been depicted in the insets of Fig. 1. The HRTEM picture (inset [B], Fig. 1) exhibits clear lattice planes implying good crystallinity inside the particle. The crystallite size of the sample is calculated from the full width of the half maximum (FWHM) of x-ray diffraction peaks using Scherrer formula.¹¹ The correction due to instrumental broadening has been taken into account.^{12,13} The calculated average crystallite size is ~ 36 nm.

III. EXPERIMENTAL RESULTS AND DISCUSSIONS

Resistivity measurement has been performed in the usual four probe method in the presence as well as absence of magnetic field. In the absence of the external magnetic field, resistivity increases with the decrease of temperature in the entire range. The large resistance below ~ 80 K exceeds the maximum measurable range of our experimental setup. The signature of transition is not visible. The application of magnetic field has a drastic effect on the transport (Fig. 2). There is a tendency of insulator to metal transition below ~ 100 K in the presence of 40 kOe magnetic field. However, complete insulator to metal transition is achieved in the presence of 60 kOe magnetic field. The temperature at which the mag-

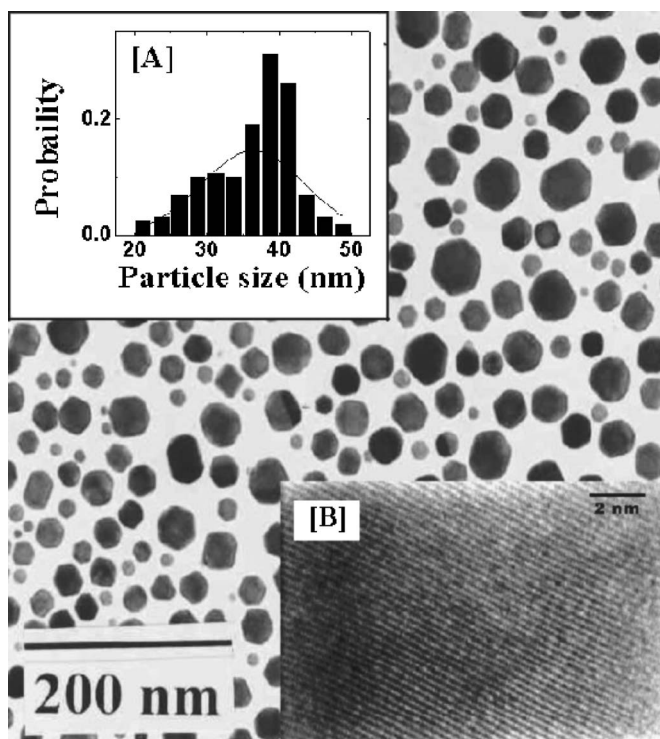


FIG. 1. Transmission electron micrograph of the nanocrystalline sample of $\text{Pr}_{0.65}\text{Ca}_{0.35}\text{MnO}_3$. Inset: [A] Histogram showing particle size distribution; [B] high-resolution transmission electron microscopy (HRTEM) image of the inside portion of a particle showing lattice resolved planes.

netic field induced insulator to metal transition occurs (T_{IM}) shifts to higher temperature with the increase of magnetic field. The transport measurements on the nanocrystalline samples indicates that the temperature dependence of resistivity (Fig. 2) in the presence as well as absence of magnetic field is almost similar to the bulk sample¹⁴ except for the invisibility of any sharp transition in the absence of magnetic field. For the bulk sample,¹⁴ the increase of resistivity at low

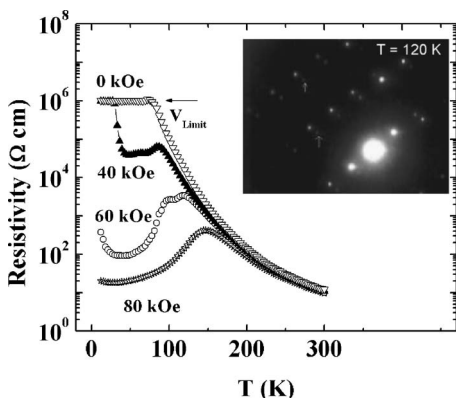


FIG. 2. Resistivity as a function of temperature for the nanocrystalline sample of $\text{Pr}_{0.65}\text{Ca}_{0.35}\text{MnO}_3$ of average particle size 50 nm in presence as well as in absence of the magnetic field. Inset: Electron diffraction pattern of selected area (SAED) of the sample at 120 K. The super lattice spots indicated by arrows are signatures of charge order transition.

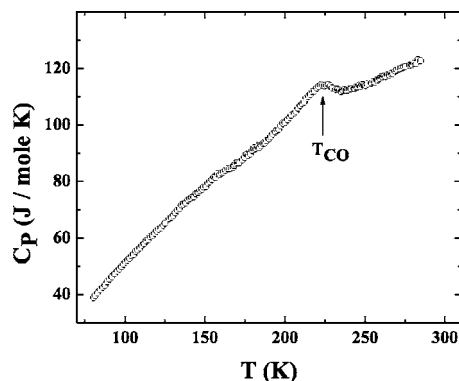


FIG. 3. Specific heat as a function of temperature for the nanocrystalline sample of $\text{Pr}_{0.65}\text{Ca}_{0.35}\text{MnO}_3$ of average particle size 40 nm in absence of the magnetic field.

temperature is due to CO. Such a high value of resistivity at low temperature for a nanocrystalline sample is expected for the existence of the CO state. The switching over of resistivity from insulating to metallic state in the presence of magnetic field may be possible due to the melting of the CO state by magnetic field for this kind of system. The shifting of T_{IM} to the high temperature region with the increase of magnetic field is also observed for the bulk sample.¹⁴

The existence of the CO state at low temperature has been further verified by electron diffraction study. In the electron diffraction pattern at low temperature, superlattice spots have been observed (inset, Fig. 2) which exist as a result of CO transition as seen in various earlier experimental studies.¹⁵⁻¹⁷

The transport measurements along with electron diffraction study clearly indicate the existence of the CO state in the case of the present nanocrystalline sample. The grain boundaries of the nanoparticles are in a disordered state and have strong extrinsic effect on transport. The intrinsic character of transition can be affected by this extrinsic effect. To get better understanding of transition, heat capacity measurement has been performed. The temperature dependence of specific heat (Fig. 3) indicates a clear peak at ~ 225 K. The temperature at which the peak is observed is almost the same as the reported charge order transition temperature (T_{CO}) of the bulk form of the sample.⁹ The peak in specific heat data in the case of the nanocrystalline sample indicates CO transition occurs at almost the same temperature as that of the bulk sample.

A commercial SQUID magnetometer has been employed to study magnetic properties of the sample. The temperature dependence of zero-field-cooled (ZFC) dc susceptibility in the presence of 1 kOe magnetic field has been shown in Fig. 4. There exists a peak around ~ 225 K (inset [A], Fig. 4), close to the reported T_{CO} of the bulk sample.⁹ The position of the peak coincides with the temperature at which the peak is obtained in the temperature dependence of specific heat. The existence of the peak is another indication of the charge order transition for the present nanoparticles. There is no clear signature of antiferromagnetic transition unlike the bulk sample. The susceptibility obeys Curie-Weiss behavior for $T > T_{\text{CO}}$ with paramagnetic Curie temperature (θ_p) ~ 157 K (inset [B], Fig. 4). The susceptibility starts to increase

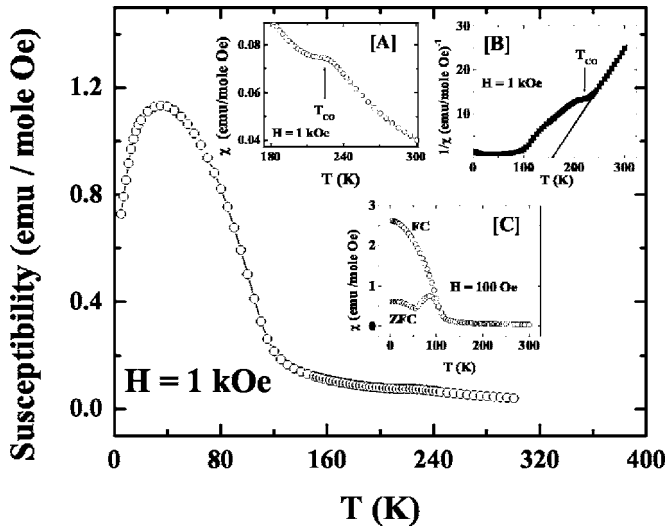


FIG. 4. The temperature dependence of zero-field-cooled dc susceptibility for the nanocrystalline sample of $\text{Pr}_{0.65}\text{Ca}_{0.35}\text{MnO}_3$. The measurements have been performed in the presence of 1 kOe magnetic field. Inset: [A] The temperature dependence of susceptibility in a high temperature region; CO transition temperature is indicated by arrow. [B] Inverse zero-field-cooled dc susceptibility at 1 kOe magnetic field has been plotted as a function of temperature. [C] The temperature dependence of zero-field-cooled and field-cooled dc susceptibility in the presence of 100 Oe magnetic field.

sharply below ~ 100 K (Fig. 4), which seems to be associated with the onset of canted antiferromagnetic (CAF) structure as observed in case of the bulk sample.⁹

The melting of CO state by magnetic field in the bulk sample is related to the CAF structure.¹⁴ The melting occurs below the temperature of the onset of CAF structure (T_{CA}).¹⁴ A similar feature has been observed for the nanocrystalline sample. The temperature T_{CA} for the nanoparticles almost coincides with that obtained for the bulk sample.⁹ At low temperature (below ~ 30 K), the susceptibility starts to drop down with the decreasing temperature as seen in the case of a similar kind of bulk sample which is believed to be a result of a spin reorientation transition¹⁸.

We have also performed the zero-field-cooled (ZFC) and field-cooled (FC) dc susceptibility measurement in the presence of the 100 Oe magnetic field (inset [C], Fig. 4). A large bifurcation between FC and ZFC curve has been observed below $\sim T_{CA}$. The surface layers of the nanoparticles are in a disordered magnetic state comprised of noncollinear spin arrangement as well as defects and vacancies. Due to the existence of this disordered surface layer, the magnetic frustration can occur and, as a result, a cluster glass state may form. The bifurcation between the ZFC and FC susceptibility curve is an indication of this glassy behavior.^{19,20}

All the measurements consistently indicate that CO transition occurs in the nanoparticles of $\text{Pr}_{0.65}\text{Ca}_{0.35}\text{MnO}_3$. The CO transition temperature in nanoparticles remains almost the same as that of the bulk form⁹ of the sample. This result directly contradicts the previous experimental results for nanocrystalline $\text{Pr}_{0.5}\text{Sr}_{0.5}\text{MnO}_3$ (Ref. 20) and $\text{Nd}_{0.5}\text{Sr}_{0.5}\text{MnO}_3$.²¹

For nanoparticles of $\text{Pr}_{0.5}\text{Sr}_{0.5}\text{MnO}_3$, ferromagnetic transition temperature (T_C) remains the same as the bulk sample

and CO transition is not observed down to 4 K.²⁰ In the case of $\text{Nd}_{0.5}\text{Sr}_{0.5}\text{MnO}_3$, T_C decreases in comparison with the bulk. However, CO transition is still invisible down to 2 K.²¹ The ferromagnetic transition is governed by DE interaction. There is no evidence of strengthening of ferromagnetic DE interaction (as reflected in the value of T_C) due to the reduction of particle size for the two samples. In spite of this fact, CO transition is hindered.²⁰ The reduction of particle size has hardly any effect on the on site Coulomb interaction.⁴ Thus there may be another factor which plays a dominant role in CO in the case of nanoparticles. Charge order transition has all the essential signatures of Martensitic transformation.⁵ During Martensitic transformation, due to the nucleation of a new crystal structure within the parent crystal, a lattice misfit arises and it gives rise to a strain known as Martensitic strain.²² This strain has to be accommodated by the system in order for the transformation to occur. The development of the Martensitic strain depends on the crystal structure of the parent phase and the Martensitic phase.²² It is not easy for nanoparticles to accommodate the Martensitic strain.^{5,22}

During the CO transition of $\text{Pr}_{0.5}\text{Sr}_{0.5}\text{MnO}_3$, the high temperature tetragonal crystal structure is changed to CO phase of monoclinic crystal structure.^{23,24} For $\text{Nd}_{0.5}\text{Sr}_{0.5}\text{MnO}_3$, CO transition is accompanied by high temperature orthorhombic crystal structure to the monoclinic crystal structure.²⁵ In both the cases, CO is associated with the transformation from the higher symmetric crystal structure to relatively lower symmetric crystal structure. On the other hand, $\text{Pr}_{0.65}\text{Ca}_{0.35}\text{MnO}_3$ transforms from orthorhombic structure to relatively higher symmetric tetragonal (pseudo) crystal structure during CO transition.²⁶ It seems that, due to the transition from lower to relatively higher crystal symmetry, the Martensitic strain developed during CO transition in $\text{Pr}_{0.65}\text{Ca}_{0.35}\text{MnO}_3$ is smaller in comparison with $\text{Pr}_{0.5}\text{Sr}_{0.5}\text{MnO}_3$ and $\text{Nd}_{0.5}\text{Sr}_{0.5}\text{MnO}_3$. As a result, the nanoparticles of $\text{Pr}_{0.65}\text{Ca}_{0.35}\text{MnO}_3$ can accommodate the strain which is rather difficult for the other two cases. The charge order transition is possible for the nanoparticles of $\text{Pr}_{0.65}\text{Ca}_{0.35}\text{MnO}_3$. However, the formation of CO state is largely affected in case of nanocrystalline $\text{Pr}_{0.5}\text{Sr}_{0.5}\text{MnO}_3$ and $\text{Nd}_{0.5}\text{Sr}_{0.5}\text{MnO}_3$. The observed behaviors of the nanoparticles of $\text{Pr}_{0.65}\text{Ca}_{0.35}\text{MnO}_3$ in the present case and $\text{Pr}_{0.5}\text{Sr}_{0.5}\text{MnO}_3$ and $\text{Nd}_{0.5}\text{Sr}_{0.5}\text{MnO}_3$ in previous cases^{20,21} show that the Martensitic-like character of the transition itself plays the dominant role in CO transition.

IV. SUMMARY

We have prepared and characterized nanoparticles of $\text{Pr}_{0.65}\text{Ca}_{0.35}\text{MnO}_3$ with average particle size ~ 40 nm. The transport, electron diffraction, heat capacity, and magnetization studies have been carried out on the sample. All the measurements indicate that the charge order transition occurs for the sample at almost the same temperature as that of the bulk form of the sample. The present experimental result leads to the conclusion that the Martensitic nature of the transition is the key factor for the occurrence of CO in a nanocrystalline sample of rare-earth manganites.

ACKNOWLEDGMENTS

The authors would like to thank Pulak Ray of Saha Insti-

tute of Nuclear Physics, Kolkata for providing TEM facility and P. V. Satyam and Jay Ghatak of Institute of Physics,

Bhubaneswar, for low temperature electron diffraction measurements.

-
- ¹ *Colossal Magnetoresistive Oxides*, edited by Y. Tokura (Gordon and Breach Science Publishers, The Netherlands, 2000).
- ² A. P. Ramirez, *J. Phys.: Condens. Matter* **9**, 8171 (1997).
- ³ J. vandenBrink and D. Khomskii, *Phys. Rev. Lett.* **82**, 1016 (1999).
- ⁴ J. vandenBrink, G. Khaliullin, and D. Khomskii, *Phys. Rev. Lett.* **83**, 5118 (1999).
- ⁵ V. Podzorov, B. G. Kim, V. Kiryukhin, M. E. Gershenson, and S.-W. Cheong, *Phys. Rev. B* **64**, 140406(R) (2001).
- ⁶ M. Uhera and S.-W. Cheong, *Europhys. Lett.* **52**, 674 (2000).
- ⁷ E. Fertman, D. Sheptyakov, A. Beznosov, V. Desnenko, and D. Khalyavin, *J. Magn. Magn. Mater.* **293**, 787 (2005).
- ⁸ A. Urushibara, Y. Moritomo, T. Arima, A. Asamitsu, G. Kido, and Y. Tokura, *Phys. Rev. B* **51**, 14103 (1995).
- ⁹ V. Dediu, C. Ferdeghini, F. C. Matocotta, P. Nozar, and G. Ruani, *Phys. Rev. Lett.* **84**, 4489 (2000).
- ¹⁰ Osami Yanagisawa, M. Izumi, W. Z. Hu, K. H. Huang, K. Nakamishi, and H. Nojima, *Physica B* **271**, 235 (1999).
- ¹¹ A. J. C. Wilson, *Proc. Phys. Soc. London* **80**, 286 (1962).
- ¹² B. E. Warren, *X-ray Diffraction* (Addison-Wesley, New York, 1969).
- ¹³ T. R. Anantharaman and J. W. Christian, *Acta Crystallogr.* **9**, 479 (1956).
- ¹⁴ Y. Tomioka, A. Asamitsu, H. Kuwahara, Y. Moritomo, and Y. Tokura, *Phys. Rev. B* **53**, R1689 (1996).
- ¹⁵ C. H. Chen and S.-W. Cheong, *Phys. Rev. Lett.* **76**, 4042 (1996).
- ¹⁶ A. P. Ramirez, P. Schiffer, S.-W. Cheong, C. H. Chen, W. Bao, T. M. Palstra, P. L. Gammel, D. J. Bishop, and B. Zegarski, *Phys. Rev. Lett.* **76**, 3188 (1996).
- ¹⁷ K. Liu, X. W. Wu, K. H. Ahn, T. Sulchek, C. L. Chien, and John Q. Xiao, *Phys. Rev. B* **54**, 3007 (1996).
- ¹⁸ M. R. Lees, J. Barratt, G. Balakrishnan, D. M. Paul, and M. Yethiraj, *Phys. Rev. B* **52**, R14303 (1995).
- ¹⁹ Zhi-Hong Wang, Tian-Hao Ji, Yi-Qian Wang, Xin Chen, Run-Wei Li, Jian-Wang Cai, Ji-Rong Sun, and Bao-Gen Shen, *J. Appl. Phys.* **87**, 5582 (2000).
- ²⁰ Anis Biswas, I. Das, and Chandan Majumdar, *J. Appl. Phys.* **98**, 124310 (2005).
- ²¹ Anis Biswas, I. Das, and R. Rawat (private communication).
- ²² *Martensitic Transition*, edited by M. Fine, M. Meshii, and C. M. Wayman (Academic, New York, 1978).
- ²³ A. Llobet, J. L. Garcia-Munoz, C. Frontera, and C. Ritter, *Phys. Rev. B* **60**, R9889 (1999).
- ²⁴ R. Kajimoto, H. Yoshizawa, Y. Tomioka, and Y. Tokura, *Phys. Rev. B* **66**, 180402(R) (2002).
- ²⁵ C. Ritter, R. Mahendiran, M. R. Ibarra, L. Morellon, A. Maignan, B. Raveau, and C. N. R. Rao, *Phys. Rev. B* **61**, R9229 (2000).
- ²⁶ Z. Jirak, S. Krupicka, V. Nekvasil, E. Pollert, G. Villeneuve, and F. Zounova, *J. Magn. Magn. Mater.* **15-18**, 519 (1980).